Lévy dusts, Mittag-Leffler statistics, mass fractal lacunarity, and perceived dimension

Raphael Blumenfeld[1] and Benoit B. Mandelbrot[2]
[1]*Theoretical Division and CNLS, Mail Stop B262, Los Alamos National Laboratory, Los Alamos, New Mexico 87545*
[2]*Mathematics Department, Yale University, New Haven, Connecticut 06520-8283*
(Received 12 June 1996)

We study the Lévy dusts on the line on two accounts: the fluctuations around the average power law that characterizes the mass-radius relation for self-similar fractals, and the statistics of the intervals between strides along the logarithmic axis (their tail distribution is related to the dust's fractal dimension). The Lévy dusts are suggested as a yardstick of neutral lacunarity, against which non-neutral lacunarity can be measured objectively. A notion of perceived dimension is introduced. We conclude with an application of the Mittag-Leffler statistics to a nonlinear electrical network. [S1063-651X(97)10202-1]

PACS number(s): 64.60.Ak

I. INTRODUCTION TO CHARACTERIZATION OF FRACTALS BEYOND THE DIMENSION: LACUNARITY, NEUTRAL LACUNARITY AS DEFINED BY ANTIPODAL INDEPENDENCE, LÉVY DUSTS, AND THEIR SAMPLING PROPERTIES

This paper uses probability theory to define a neutral fractal lacunarity and suggests a way to measure lacunarity when it is not neutral. Critical percolation clusters, for example, are of neutral lacunarity and will be studied elsewhere. Several papers discussed lacunarity and its concrete uses. But the topic is still new and unfamiliar, therefore we shall begin by addressing the fundamental issues.

Visual lacunarity. Consider the Cantor dusts stacked in Fig. 1 reproduced from [1]. These dusts share the same fractal dimension, $D=1/2$, but differ in an obvious manner. Those at the stack's bottom have small holes, can be described as fine grained, and mimic filled-in intervals. In Ref. [2] they are termed *low lacunarity*. Those at the stack's top have big holes, can be described as coarse grained, and mimic two dots; they are termed *high lacunarity*. This demonstrates a general point; a set with a given fractal dimension D can be made to mimic a broad range of quite different textures, pointing to the fact that the fractal dimension is not enough to uniquely characterize fractals.

There is a strong need to measure quantitatively the differences in lacunarity between textures in self-similar physical structures, such as galaxy distributions, spin domains in magnetic systems, diffusion-limited aggregates, microstructures of porous and composite materials, and so on. Fourier analysis and spectral characterization only give the fractal dimension. It would be convenient if the quantitative lacunarity to quantify these differences would take the value 0 in those cases where the lacunarity can sensibly be said to be ''neutral,'' i.e., right on the boundary between high and low.

The main goal of this paper can now be sketched. A fractal of non-neutral lacunarity seems to the eye to have an apparent fractal dimension different from the actual value. Therefore, we shall investigate fractal dusts on the line and define for them a quantity that will be denoted by D_P and called ''perceived dimension.'' This is *not* a fractal dimension, but the eye trained on Lévy dusts may perceive it as one. The perceived dimension can be higher or lower than the fractal dimension, depending on lacunarity. Dimensions must not be multiplied beyond necessity (and they have already multiplied beyond comfort), but necessity has arisen again. In effect, D_P measures how low or high a given fractal sits on a stack such as that illustrated in Fig. 1.

These issues raise a few difficulties: (a) The notion of lacunarity turns out to be many sided, giving rise to several distinct definitions. As a matter of fact, this paper will discuss two versions of a concept one may call *fluctuation lacunarity*. (b) Some of those definitions (but not D_P) fail to define a neutral state. (c) All definitions are statistical. For example, while the Cantor dusts illustrated in Fig. 1 are generated by a deterministic mechanism, typical empirical studies may involve, instead of a full dust in (0,1), a piece contained between two points randomly selected in time; such a piece is a random set. In the random context, each measure of lacunarity is a function of a sample of observations. That is, even when the true lacunarity is neutral, with typical value 0, the value actually measured on a sample is a random variable. Hence, the difference between measurements made on samples of two distinct fractals will reflect not only the difference between true lacunarities, but also a sampling error.

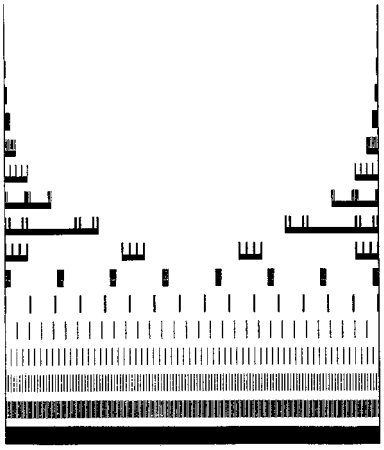

FIG. 1. A stack of Cantor sets of equal dimension $D=1/2$, whose lacunarity changes from very low at the bottom to very high at the top of the stack.

The mass-radius relation, its prefactor F, the prefactor's variability factor, and a measure of lacunarity. Given a ball of radius R in E dimensions, which encloses a self-similar fractal structure, the total mass (measure) $M(R)$ enclosed by the ball is known [2] to take the form

$$M(R)=FR^{D} \tag{1.1}$$

or

$$\ln M(R)=\ln F+D\ln R.$$

The exponent D is the fractal dimension and is smaller than the embedding Euclidean dimension E. In the case of the Lévy dust, the prefactor F is a random variable independent of R. For both F and $\ln F$, we obtain the expectation, variance, and other statistical properties. Operatively, the distribution of the prefactor F can be constructed by moving the origin of a ball of radius R throughout the structure, measuring the mass enclosed by the ball, and repeating the procedure for many values of R. The existence of a well-defined F independent of R presupposes that the structure is self-similar with respect to all reduction ratios r, and hence calls for description as a random fractal. A systematic fractal such as the Cantor dust is self-similar with respect to reduction ratios r that fall into a geometric sequence (such as 4^{-h} in Fig. 1); it follows that F is a noisy function that is roughly periodic with period $\ln R$ [3].

The prefactor F, or even its expectation, received far less attention in the literature than the scaling exponent D. The importance of F resides in its intimate connection to the concept of lacunarity. To understand why, note that the ensemble average relation (1.1), $\langle M(R)\rangle=\langle F\rangle R^{D}$, is in effect the density-density correlation function of the structure multiplied by R^{E}. In translationally invariant systems, the density-density correlation function gives information on the mass fluctuations, and hence on texture, but due to the dilation symmetry of fractals, this function only yields the quantity F and the scaling exponent of the average mass. Since, as we have already noted, a fractal structure cannot be described only by its dimension, one signature beyond simple scaling is the statistical variability (to be defined below) of $M(R)$ for fixed R. Intuitively, this variability ought to be smaller in a fine-grained structure than in a coarse-grained one. Hence, a possible signature of lacunarity is the ratio of the variance to the square of the expectation, as measured for either F or $\ln F$.

The Lévy dust as a yardstick of neutral lacunarity; antipodal correlation. The least structured or ''most relaxed'' of all point distributions on the line is the Lévy dust, which is generated as the set of positions of an increasing Lévy flight. The successive steps in a flight follow the distribution $\Pr\{U\geq u\}=u^{-D}$, and are independent. Therefore, the Lévy dust L has the property that, if the origin Ω belongs to L, the portions of the dust to the right and the left of Ω are statistically independent. Those opposite directions are denoted by the term ''antipodal.'' One of us [2] observed that a positive correlation between those halves is perceived as low lacunarity and a negative correlation is perceived as high lacunarity. It follows that the Lévy dust is a useful standard of *neutral lacunarity*. It was shown [4] that linear cuts through critical percolation and Ising clusters are of neutral lacunarities. See also [5]. This motivated us to investigate the Lévy dusts deeper, from viewpoints that did not previously seem compelling. The generalization to fractals embedded in higher dimensions is not straightforward and will be presented elsewhere.

This paper is constructed as follows. Section II introduces the Lévy flight process and the resultant Lévy dust. The reduced mass $M(R)R^{-D}$ for the Lévy dust is a Feller-Mittag-Leffler (FML) random variable and we discuss its properties and plot its distribution (apparently, for the first time). Section III uses the ratio of variance to squared expectation of the FML random variable to define the perceived dimension D_p. We mention in Sec. III generalizations concerning higher cumulants of the FML distribution. Section IV addresses the distribution of the logarithm of the Feller-Mittag-Leffler variable, and discusses its properties and its bilateral Laplace transform. We show how its Fourier transform yields an accurate measure of the fractal dimension. Section V analyzes the distribution of strides on the $\ln R$ axis, which is closely related to the Lévy-flight process. We show that this distribution possesses a rich and instructive behavior and we present numerical results in support of our predictions. Section VI demonstrates the applicability of the Mittag-Leffler statistics to a nonlinear electrical network. We conclude in Sec. VII by discussing some implications of our results and possible new directions.

II. THE LÉVY FLIGHT AND THE FELLER-MITTAG-LEFFLER RANDOM VARIABLES AND PROCESSES

In the following, we shall adopt the probabilists' notations, denoting random variables by upper-case letters and their values by the corresponding lower-case letter. For $0<D<1$, a truncated Lévy flight process on the line is as follows [1]: Start with a uniform distribution in the range $(\epsilon,1)$, where $\epsilon\to 0^{+}$, and choose an array of M ordered numbers u_i $(i=1,2,\ldots,M)$. From this array form the following sequence of numbers V_m:

$$V_m=\sum_{i=1}^{m} U_i^{-1/D} \quad (m=1,2,\ldots,M), \quad 0<D<1. \tag{2.1}$$

The collection of the points $V_m>0$ on the positive half line constitutes a truncated Lévy dust. It is known that, in the limit $\epsilon\to 0$, the number of these points within a distance R from the origin satisfies Eq. (1.1).

The FML distribution. It is known [6] that the random prefactor F follows the Mittag-Leffler distribution, whose probability density is

$$\mu_D(f)=\frac{1}{\pi}\sum_{k=1}^{\infty}\frac{(-1)^{k-1}}{(k-1)!}\sin(\pi kD)\Gamma(kD)f^{k-1},$$

$$0<f<\infty. \tag{2.2}$$

The Mittag-Leffler distribution was first observed by Will Feller, who chose this name because the generating function of $\mu_D(f)$ is the Mittag-Leffler function:

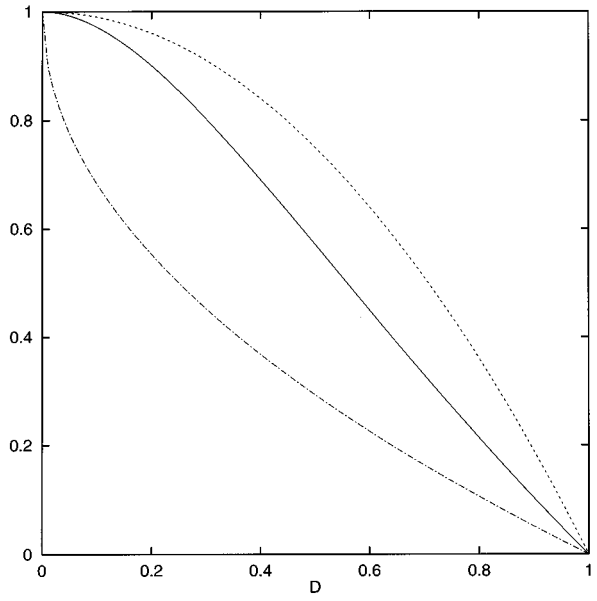

FIG. 2. The variability factor $\Phi(D)$ for the Lévy flight (solid line). The dotted (dash-dotted) line is an example of systems with perceived dimensions, D_P higher (lower) than D and hence with lacunarity which is below (above) neutral.

$$\mathcal{L}(t|\mu_D)=\int_0^\infty e^{-tf}\mu_D(f)\,df=\sum_{k=0}^{\infty}\frac{(-t)^k}{\Gamma(1+kD)}. \quad (2.3)$$

We hope that our denotation here will restore to W. Feller some credit that he deserved but chose not to claim. A few properties of this distribution were known [7]: for $D\to 0$, $\mu_D(f)\to\exp(-f)$; for $D=1/2$, $\mu_D(f)$ is a half-Gaussian; and, for $D\to 1$, $\mu_D(f)$ approaches the δ function. The form of (2.3) indicates that the integer m-th moments of $\mu_D(f)$ are

$$\langle f^m\rangle=\frac{m!}{\Gamma(1+mD)}. \quad (2.4)$$

The FML random processes. The reduced mass $F=M(R)R^{-D}$ can be considered a function of R. Its marginal distribution for given R is a FML distribution, whose sample functions in time to our knowledge have not been investigated until now. We think that they deserve to be called FML random functions.

III. LACUNARITY AS DEFINED THROUGH THE MASS VARIABILITY, AND THE CONCEPT OF ''PERCEIVED DIMENSION''

The variability factor. A possible second-order characterization of lacunarity is the variability factor [8]

$$\Phi(D)\equiv\frac{\langle(f-\langle f\rangle)^2\rangle}{\langle f\rangle^2}=\frac{\langle f^2\rangle}{\langle f\rangle^2}-1. \quad (3.1)$$

From Eq. (2.4) we find

$$\Phi(D)=\frac{2\Gamma^2(1+D)}{\Gamma(1+2D)}-1,$$

which is plotted in Fig. 2 against D.

The variability factor is independent of R due to the self-similarity of the Lévy dust, and is related to the fact that the jumps of the Lévy flight have an infinite expectation. For the stopovers of a flight in which the jumps have a finite expectation, the variability factor Φ depends on R, and tends to 0 as $R\to\infty$, which is a restatement of the law of large numbers. (For example, in a Poisson process, the variability factor varies as R^{-1}.) For the Lévy dust, the factor $\Phi(D)$ is independent of R and decreases monotonically with the fractal dimension D. For example, $\Phi(D\to 0)\to 1$ for $\Phi(D=1/2)=\pi/2-1=0.5708$, and $\Phi(D\to 1)\to 0$.

It was to be expected that, for the Lévy dust, the value of this lacunarity should depend strongly on the fractal dimension. Indeed, a Lévy dust near $D=1$ is almost uniformly distributed and the variability factor of its mass, $M(R)$, should be small. On the other hand, a Lévy dust with $D\ll 1$ is extremely uneven and the variability factor of its $M(R)$ has to be very large. The graph of $\Phi(D)$ confirms that for Lévy dusts lacunarity increases as D goes from 1 to 0. It also shows that $\Phi(D)$ is very sensitive to D near $D=1$, where $\Phi'(1)=-1$, and not at all sensitive near $D=0$, where $\Phi'(0)=0$. Therefore, the techniques to be advanced below are better suited for values of D that are not very small compared to 1.

The perceived dimension. Let us consider now the Cantor stack shown in Fig. 1. When the lacunarity is far lower than neutral, the set mimics a filled-in interval. That is, it mimics a misleadingly higher value of D. This in turn means that one expects the variability factor to be smaller than the true value of $\Phi(D)$.

The function $\Phi(D)$ suggests then a perspicuous way to measure lacunarity. Invert the function $\Phi(D)$ for the Lévy dust, Eq. (3.1), to obtain a function $D_N(\Phi)$, where the index N refers to the neutral character of the Lévy dust. From the measured histogram of F for any given real system obtain the measured value of Φ. Now insert the measured value of Φ into the function $D_N(\Phi)$. The result can be called a (visually) ''perceived dimension,'' which we denote by D_P. The three possibilities that arise are interpreted as follows: When $D_P=D$, the lacunarity is defined as neutral; when $D_P>D$, the lacunarity is defined below neutral; when $D_P<D$, the lacunarity is defined above neutral.

Thus, one can take the value of D_P as a measure of lacunarity. For example, suppose that in Fig. 2 the dotted and dash-dotted lines represent a set of measurements of the systems' variability factors. The entire dotted (dash-dotted) line shows a perceived dimension higher (lower) than D and therefore its lacunarity is below (above) neutral. Note that this measure provides a different scale for each true D, a complication that may be avoided by taking the ratio of perceived to true dimension, D_P/D [or perhaps, $D_P/(1-D)$], but we have not yet explored this idea.

Higher order variability factors. Once again, the main significance of $\Phi(D)$ in measurements of self-similar random data is that it helps distinguish different fractals with the same, or similar, values of D but different structure (lacunarity). One can generalize the above analysis to orders higher than second and define the following families of quantities,

$$S_k(D)\equiv\frac{C_k(D)}{[C_1(D)]^k}. \quad (3.2)$$

TABLE I. Values of S_k for $k=2,3,4$ at $D\to 0$, 1/2, 1.

D	$S_2=\Phi(D)$	S_3	S_4
$D\to 0$	1	2	6
$D=1/2$	$\pi/2-1$	$2-\sqrt{2}/\pi$	$2\pi-6$
$D\to 1$	0	0	0

In this expression $C_k(D)$ is the kth cumulant of the FML distribution. Clearly, $S_2(D)=\Phi(D)$. It is straightforward to show that $S_k(D)$ is a decreasing function of D for all k. For example, for $D\to 0$, 1/2 and 1 and $k=2$, 3, and 4 we find the values given in Table I. For all k, in the limit $D\to 0$, $S_k\to(k-1)!$ and when $D\to 1$, $S_k\to 0$.

IV. THE LOGARITHMIC MITTAG-LEFFLER DISTRIBUTION

The traditional way to analyze fractal structures is to plot $\ln m$ against $\ln V_m$, which yields the fractal dimension as the average slope of the resultant line. After this linear line has been subtracted, the plot of $\ln F$ as function of $\ln R$ resembles a noisy time series. Figure 3 shows a typical plot of such a process with $D=0.2$. It is therefore natural to call $\ln F$ the logarithmic Mittag-Leffler (LML) random variable.

Consider the random variables Y and $\tilde{R}$ defined through

$$\tilde{R}=\ln R,$$

$$Y=\ln F=\ln M-D\ln R.$$

Using Eq. (2.2), the probability density of Y is

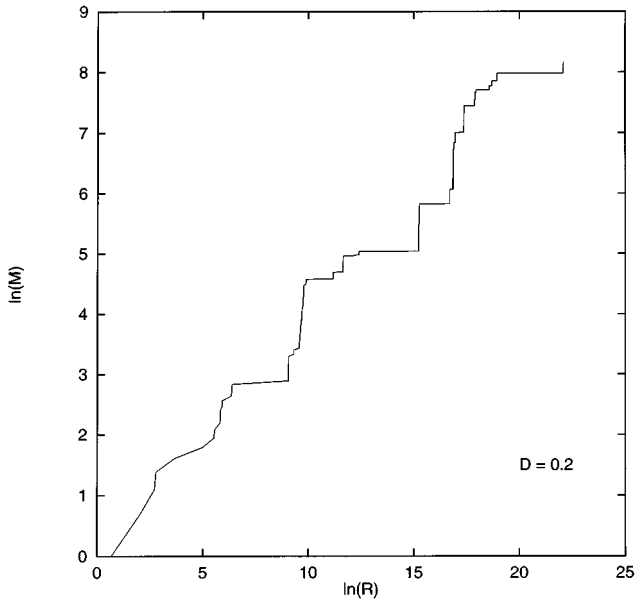

FIG. 3. A typical plot of the mass logarithm vs the radius logarithm (both natural logarithms). The fractal dimension in this plot is $D=0.2$.

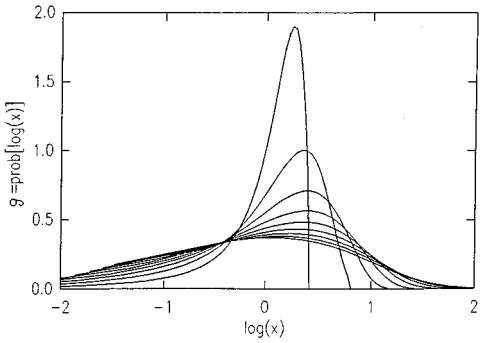

FIG. 4. The logarithmic Mittag-Leffler probability density against $\log_2(x)$ for $D=0.1$–0.9 in steps of 0.1. The highest peak belongs to the curve with $D=0.1$.

$$g_D(y)=\mu_D(f=e^y)\left|\frac{df}{dy}\right|_{f=e^y}$$

$$=\frac{e^y}{\pi}\sum_{k=1}^{\infty}\frac{(-e^y)^{k-1}}{(k-1)!}\sin(\pi kD)\Gamma(kD), \quad (4.1)$$

where $-\infty<y<\infty$.

Numerical evaluation and unimodality. Figure 4 plots $g(y)$ for values of D that range from $D=0.1$ to $D=0.9$ in steps of 0.1. These plots are obtained by numerical evaluation of the sum in Eq. (4.1), cut off at a value $k_{\max}$ beyond which the remainder of the sum can be neglected.

For all D, $g_D(y=\infty)=0$. Since $g_D(y)$ is not constant, there exists at least one y^* for which $g(y^*)$ is a maximum, i.e., $g_D(y^*)\geq g_D(y)$ for all y. It can be shown very easily that for $D\to 1$, 1/2, y^* is unique, so that $g(y)$ is unimodal. Indeed, by plotting $g(y)$ for many values of D between 0 and 1 (Fig. 4) we find that this result holds for all D in this range.

The bilateral Laplace transform and related analytic results. The bilateral Laplace transform of $g_D(y)$ is

$$\mathcal{L}(t|g_D)=\int_{-\infty}^{\infty}e^{ty}g_D(y)dy=\frac{\Gamma(1+t)}{\Gamma(1+tD)} \quad (4.2)$$

for any positive and integer value of t. The right-hand side of Eq. (4.2) is obtained by substituting the form (4.1) in the integral and changing variables to $f=e^y$. The proof that the resulting integral is exactly the tth moment Eq. (2.4) is straightforward and uses Eqs. (2.2) and (2.4). For *complex* values $t=\theta+i\tau$ (provided that the integral for the moment exists), we use the generalized form of the gamma function [9], and relation (4.2) becomes

$$\mathcal{L}(\theta+i\tau|g)=\frac{\Gamma(1+\theta+i\tau)}{\Gamma(1+(\theta+i\tau)D)}, \quad (4.3)$$

which for $\theta=0$ is the bilateral Fourier transform. Using [9], the spectral intensity is

$$|\mathcal{F}(\tau|g)|^2=\frac{1}{D}\frac{\sinh(\pi\tau D)}{\sinh(\pi\tau)}. \quad (4.4)$$

Relation (4.4) is easy to check for the three values of D where the FML is known explicitly. Integrating over the

$(i\tau)$th moment $\mathcal{F}(\tau|g)=\int_0^\infty f^{i\tau}\mu_D(f)df$ immediately yields Eq. (4.4) for these three values.

Direct relevance of relation (4.4) to practical measurements of D. For small values of τ we find, by expanding relation (4.4),

$$|\mathcal{F}(\tau|g)|^2\sim 1-(1-D)^2\,\frac{\pi^2}{6}\,\tau^2\sim\exp\{-\pi^2\tau^2(1-D^2)/6\}. \tag{4.5}$$

Whenever τ is not very small, such that $\exp(2\pi\tau D)$ is not very close to 1, we obtain

$$\ln(|\mathcal{F}(\tau|g)|^2)\sim\text{const}\times[-\pi(1-D)\tau]. \tag{4.6}$$

Thus, plotting the intensity $|\mathcal{F}(\tau|g)|^2$ semilogarithmically it should be possible to observe a constant slope for $\tau>1/(2\pi D)$, which extends over a wide range of values of τ. For small values of τ $(\gg\sqrt{6}/[\pi(1-D)])$, this plot should be decreasing parabolically. It follows that relations (4.6) and (4.7) allow one to cross determine the dimension of the system. Given a system whose fractal dimension is unknown, all we need to do is construct the histogram of the random variable Y and then Fourier transform it. Plotting the logarithm of the absolute square (the intensity) of the Fourier coefficient as a function of τ should give, away from the origin, a straight line of slope $\pi(1-D)$ as in Eq. (4.6). This method can be used to check on the traditional method of plotting $\ln m$ versus $\ln(R_m)$. Furthermore, this technique may be more accurate for systems that are not large enough for the usual mass averaging. Therefore its applicability is more promising at low fractal dimensions ($D\ll 1$). We will pursue this issue in Sec. V.

V. THE DISTRIBUTION OF THE RELATIVE JUMPS IN THE RADIUS

Self-similarity concerns dilation or reduction, which are multiplicative operations. Taking logarithms transforms them into translations. A particular application of such a transformation to logarithmic coordinates is discussed in [3]. For example, take the standard Cantor dust on [0,1], extrapolate it to the right by successive expansions of ratio 3, and look at it in the coordinate $\tilde{\tau}=\ln\tau$. When the dust is infinitely interpolated, its image in ln(time) is a periodic point process on the whole line, in which large gaps of length ln 2 alternate with deformed Cantor dusts of length ln(3/2). Now, consider a truncated dust, i.e., one interpolated down to a smallest ''atom,'' but no further. Its image in ln(time) is a process on the half-line to the right of the origin. The successive large gaps are unchanged by the imposition of an inner cutoff, and the successive pieces between the gaps build up as one moves right to an infinitely interpolated deformed Cantor dust. In that limit, the distribution of the gap lengths converge to a well-defined limit. For small gap lengths, this limit is $\Pr(V>u)\sim u^{-D}$.

Let us return to our random Lévy dust. Once again, in logarithmic coordinates the dust transforms into a stationary random point process. In other words, the quantity

$$\rho_m=V_m-V_{m-1}=\ln\left[1+\frac{u_m^{-1/D}}{\sum_{i=1}^{m-1}u_i^{-1/D}}\right] \tag{5.1}$$

has a limit distribution independent of m. We reiterate that the FML random process $M(R)R^{-D}$ can be viewed as function of $\ln R$ and it becomes a Feller-Mittag-Leffler process in this variable. The random variable ρ_m is the difference between the mth and the $(m-1)$th steps on the logarithmic axis on which the Lévy dust was mapped. In practice, as we know, the values of u_i are picked from a uniform probability density that ranges from $u_{\min}=\epsilon>0$ to $u_{\max}=1$. A lower cutoff is required by both physics and computational constraints. We stress that the results are independent of ϵ, which simply facilitates the calculations. Thus the probability density of u_i is

$$f(u_i)=\begin{cases}1/(1-\epsilon), & \epsilon<u_i<1\\ 0, & \text{otherwise.}\end{cases} \tag{5.2}$$

We now seek the probability density of the variable $\nu_m=\exp(\rho_m)$. The probability density of ν, $\tilde{P}(\nu)$, can be found through

$$\begin{aligned}\tilde{P}(\nu_m)&=\int_0^\infty\left(\prod_{i=1}^m f(u_i)du_i\right)\delta\left[\nu_m-\left(1+\frac{u_m^{-1/D}}{\sum_{i=1}^{m-1}u_i^{-1/D}}\right)\right]\\&=\left(\frac{D}{1-\epsilon}\right)^m\int_1^{\epsilon^{-1/D}}\left[\prod_{i=1}^{m-1}\omega_i^{-(D+1)}d\omega_i\right]\\&\quad\times\left[(\nu_m-1)\sum_{i=1}^{m-1}\omega_i\right]^{-(D+1)}.\end{aligned} \tag{5.3}$$

Using the normalization condition and some algebra we find that

$$\tilde{P}(\nu_m)=\frac{\epsilon D}{(1-\epsilon^2)(m-1)^D}\,(\nu_m-1)^{-(D+1)} \tag{5.4}$$

The next step is to obtain the probability density of ρ_m:

$$\begin{aligned}P(\rho_m)&=\left[\tilde{P}(\nu_m)\,\frac{d\nu_m}{d\rho_m}\right]_{\nu_m=\exp(\rho_m)}\\&=\frac{\epsilon D}{(1-\epsilon^2)(m-1)^D}\,\frac{e^{\rho_m}}{(e^{\rho_m}-1)^{D+1}},\end{aligned} \tag{5.5}$$

where ρ_m is defined over the interval

$$(\ln[1+\epsilon^{1/D}/(m-1)],\ln[1+\epsilon^{-1/D}/(m-1)]),$$

which tends to $(0,\infty)$ as $\epsilon\to 0$. This probability density decreases monotonically with ρ_m from its maximal value of

$$P_{\max}=\frac{D}{1-\epsilon^2}\,[(m-1)\epsilon^{-1/D}+1] \tag{5.6}$$

at the lowest value of ρ_m. Moreover, P is a strictly convex function of its argument; a property that can be verified by considering the signs of successive derivatives of P: In terms of $t\equiv e^{\rho_m}-1$, Eq. (5.5) becomes

$$P(t)=P_0(t^{-D}+t^{-D-1}), \quad P_0=\frac{\epsilon D}{(1-\epsilon^2)(m-1)^D}. \tag{5.7}$$

The sign of the kth derivative, $d^{(k)}P(\rho_m)/d\rho_m^k$, is the same as that of $d^{(k)}P(t)/dt^k=(-1)^k$. This change of sign with successive differentiations shows that $P(\rho_m)$ is strictly convex.

In the plot of the logarithm of $P(\rho_m)$ as a function of $t_m=\exp(\rho_m)-1$, it should be possible to detect the combination of the two slopes $-D$ and $-D-1$ in expression (5.7). At low values of t_m (i.e., ρ_m very close to zero) the mean slope is $-D-1$ and it crosses over to $-D$ for large values of t_m. This distribution plays an important role in many physical systems and the tail of the cumulative distribution of the variable ρ_m, $G(\tilde{\rho})$, is

$$G(\tilde{\rho})=\int_{\ln\tilde{\rho}}^{\infty}P(\rho_m)d\rho_m=\frac{\epsilon}{1-\epsilon^2}\,[(\tilde{\rho}-1)^{-D}(m-1)^D-\epsilon]. \tag{5.8}$$

Since the behavior is not purely exponential in $\ln\tilde{\rho}$ there appears a crossover when the first term in the curly brackets becomes comparable to ϵ. This can be understood by inspecting relation (5.8): as D decreases, the first term in the curly brackets decreases and for a given value of ϵ the two terms become comparable for larger values of $\tilde{\rho}$.

VI. THE FML IN A SYSTEM OF NONLINEAR VARISTORS

The Mittag-Leffler statistics have many interesting applications in physical systems, most of which have not yet been recognized or addressed. Here we give an illustrative example of one such application: the occurrence of the FML distribution in a conducting system of varistors. A varistor is a nonlinear resistor that follows a current-voltage characteristic of the form [10]

$$V_j=r_jI_j^{\alpha}, \tag{6.1}$$

where V_j and I_j are, respectively, the voltage drop and the current pertaining to the jth varistor r_j is a coefficient, which we term resistance due to its being parallel to the usual linear resistance, but whose units are $\Omega/\mathrm{A}^{\alpha-1}$. The parameter α (which is usually temperature dependent) is presumed constant for all the varistors in the structure. We shall limit our discussion to the sublinear regime $0<\alpha<1$. We consider m varistors connected in parallel between two nodes A and B as in Fig. 5,

$$V_{AB}=R_{AB}I_{AB}^{\alpha}. \tag{6.2}$$

The question that we address is how R_{AB} is distributed. For a given realization of the local variables r_j, the value of R_{AB} is given exactly by

$$R_{AB}=\left(\sum_{j=1}^{m}r_j^{-1/\alpha}\right)^{-\alpha}. \tag{6.3}$$

The direct equivalence between relations (6.3) and (2.1) is immediately apparent via the transformations

$$\alpha\leftrightarrow D, \quad r_j\leftrightarrow u_j, \quad V_m\leftrightarrow R_{AB}^{-1/\alpha}.$$

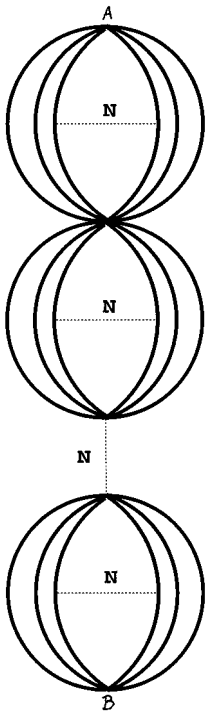

FIG. 5. A varistors electric circuit realization of Mittag-Leffler variables and statistics.

Substituting these into Eq. (1.1) yields

$$R_{AB}=F/m, \tag{6.4}$$

and it follows that R_{AB} is a FML random variable with $\mu_\alpha(f)$ [see Eq. (2.2)]. For example, the average of R_{AB} is

$$\langle R_{AB}\rangle=1/[m\Gamma(1+\alpha)]. \tag{6.5}$$

Similarly, the second moment of this distribution is

$$\langle\delta R_{AB}^2\rangle=\langle R_{AB}^2\rangle-\langle R_{AB}\rangle^2=\frac{2}{m\Gamma(1+2\alpha)}-\frac{1}{m^2\Gamma^2(1+\alpha)}, \tag{6.6}$$

and so on. Thus the above analysis directly applies to this system and one can learn about the statistics of the nonlinear conducting system by adapting relations from the Lévy dust statistics.

It should be mentioned that the same calculation can be applied to *continuous* nonlinear dielectrics with slabs in parallel or perpendicular to the capacitor plates, since the expression for the total dielectric constant has exactly the same form as Eq. (6.3) [11].

VII. CONCLUSION

Characterization of fractal structures by lacunarity is a much needed step beyond description by a fractal dimension. It is difficult to know from measuring a seemingly random structure what is the process that generated it. Further, even if the process was known, the structure's statistics are usually difficult to analyze. Therefore, it is of value to have a baseline system, whose mass distribution is well understood, and against which lacunarities of other fractal processes can be

compared and classified. We propose the Lévy dust for this role. Since the Fourier transform of the LML distribution is known explicitly, one can analyze the spectrum of a measured stochastic process at hand and compare with the Lévy dust. The similarities and differences can then yield information about the rules that generated the observed structure.

We addressed in detail the lacunarity of the Lévy dust and generalized the definition of lacunarity given in [8] to higher order cumulants of the distribution of $\ln F$ obtaining a family of related quantities S_k for the Lévy dust, the S_k depend only on the fractal dimension D. This confirms that lacunarity cannot reduce to one number but requires several measurements that are mutually dependent in subtle ways.

We also discussed the distribution of the strides between the mth and the $(m-1)$th steps along the $\ln R$ axis, and found its tail distribution. This tail is directly related to the apparent self-similarity and gives another possibility to measure the fractal dimension. The advantage of this method of determining D is in its robustness against errors due to too small statistics and hence is valuable for low values of D, where traditional approaches need gathering of many points, resorting to very large data sets.

It should be emphasized that F and S_k are not the only possible characterizations of lacunarity. See, e.g., Refs. [3] and [4]. For Cantor dusts and other highly hierarchical structures, $M(R)R^{-D}$ is not a random variable independent of R, but rather a noisy periodic function of $\ln R$ [3] and the notion of lacunarity becomes more involved. Such a log-oscillatory behavior occurs, for example, in fracture sidebranching [12] and in many biological branching systems. The notion of lacunarity is also beginning to play a central role in the study of diffusion-limited aggregation [13]. A related approach to lacunarity [4] concerns the statistics of antipodal correlations about points in the structure. In one dimension, for example, this consists of correlations between ''forward'' and ''backword'' structures. The connection between this and our approach deserves a careful look.

ACKNOWLEDGMENTS

R.B. acknowledges helpful discussions with A. Aharony, Y. Gefen, F. Guder, A. R. Bishop, and thanks the IBM T. J. Watson Research Center, Yorktown Heights, and Harvard University for hospitality and support. J. S. Lew and D. Quarles helped with the numerical work and estimated $k_{\max}$ for us in Eq. (4.1).

[1] B. B. Mandelbrot, in *Fractal Geometry and Stochastics*, edited by C. Bandt, S. Graf, and M. Zähle (Birkhäuser, Basel, 1995), pp. 12–38; See also in *Fractals in Biology and Medicine*, edited by T. F. Nonnenmacher, G. A. Losa, and E. R. Weibel (Birkhäuser, Basel, 1993), p.8 .

[2] B. B. Mandelbrot, *The Fractal Geometry of Nature* (Freeman, New York, 1982) pp. xii, 461, xvi.

[3] R. Blumenfeld and R. C. Ball, Phys. Rev. E **47**, 2298 (1993); Fractals **1**, 985 (1993).

[4] B. B. Mandelbrot and D. Stauffer, J. Phys. A **27**, L237 (1994); see also B. B. Mandelbrot, R. Pastor-Satorras, and E. Rausch (unpublished).

[5] J. P. Hovi, A. Aharony, D. Stauffer, and B. B. Mandelbrot, Phys. Rev. Lett. **77**, 877 (1996). See also B. B. Mandelbrot (unpublished).

[6] W. Feller, Trans. Am. Math. Soc. **67**, 98 (1949).

[7] B. B. Mandelbrot, in *Proceedings of the Fifth (1965) Berkeley Symposium on Mathematical Statistics and Probability*, edited by L. LeCam and J. Neyman (University of California Press, Berkeley, CA, 1967), pp. 3, 155–179.

[8] Y. Gefen, B. B. Mandelbrot, Y. Meir, and A. Aharony, Phys. Rev. Lett. **50**, 145 (1983).

[9] See, e.g., Abramowitz and I. A. Stegun, *Handbook of Mathematical Functions* (Dover, New York, 1972).

[10] R. Blumenfeld and A. Aharony, J. Phys. A **18**, L443 (1985); R. Blumenfeld, Y. Meir, A. Aharony, and A. B. Harris, Phys. Rev. B **35**, 3524 (1987).

[11] R. Blumenfeld and D. J. Bergman, Phys. Rev. B **44**, 7378 (1991).

[12] R. C. Ball and R. Blumenfeld, Phys. Rev. Lett. **65**, 1784 (1990); R. C. Ball, P. W. H. Barker, and R. Blumenfeld, Europhys. Lett. **16**, 47 (1991).

[13] B. B. Mandelbrot, Physica A **191**, 95 (1992); B. B. Mandelbrot, H. Kaufman, A. Vespignani, I. Yekutieli, and C.-H. Lam, Europhys. Lett. **29**, 599 (1995); B. B. Mandelbrot, A. Vespignani, and H. Kaufman, *ibid*. **32**, 199 (1995).